

# Inelastic $J/\psi$ Production in Deep Inelastic Scattering from Hydrogen and Deuterium and the Gluon Distribution of Free Nucleons

THE NEW MUON COLLABORATION (NMC)

Bielefeld University<sup>1+</sup>, CERN<sup>2</sup>, Freiburg University<sup>3+</sup>, Max-Planck Institute Heidelberg<sup>4</sup>, Heidelberg University<sup>5+</sup>,  
Indiana University<sup>6</sup>, University of Mainz<sup>7+</sup>, Mons University<sup>8</sup>, Neuchâtel University<sup>9</sup>, NIKHEF- K<sup>10++</sup>,  
Oxford University<sup>11</sup>, University of California, Santa Cruz<sup>12</sup>, PSI<sup>13</sup>, Torino University and INFN Torino<sup>14</sup>,  
Uppsala University<sup>15</sup>, Institute for Nuclear Studies, Warsaw<sup>16\*</sup>, Warsaw University<sup>17\*\*</sup>, Wuppertal University<sup>18+</sup>

D. Allasia<sup>14</sup>, P. Amaudruz<sup>13a)</sup>, M. Aমেদো<sup>14</sup>, A. Arvidson<sup>15</sup>, B. Badelek<sup>17</sup>, G. Baum<sup>1</sup>,  
J. Beaufays<sup>10b)</sup>, I.G. Bird<sup>4</sup>, M. Botje<sup>13</sup>, C. Broggini<sup>9</sup>, W. Brückner<sup>4</sup>, A. Brüll<sup>3</sup>, W.J. Burger<sup>13</sup>,  
J. Ciborowski<sup>10</sup>, R. Crittenden<sup>6</sup>, R. van Dantzig<sup>10</sup>, H. Döbbling<sup>4c)</sup>, J. Domingo<sup>13d)</sup>, J. Drinkard<sup>12</sup>,  
A. Dzierba<sup>6</sup>, H. Engelen<sup>3</sup>, M.I. Ferrero<sup>14</sup>, L. Fluri<sup>9</sup>, P. Grafstrom<sup>15e)</sup>, E. Hagberg<sup>15</sup>, D. von Harrach<sup>4f)</sup>,  
M. van der Heijden<sup>10</sup>, C. Heusch<sup>12</sup>, Q. Ingram<sup>13</sup>, A. Jacholkowska<sup>6g)</sup>, K. Janson<sup>15</sup>, M. de Jong<sup>10</sup>,  
E.M. Kabu<sup>4</sup>, R. Kaiser<sup>3</sup>, T.J. Ketel<sup>10</sup>, F. Klein<sup>7</sup>, B. Korzen<sup>18</sup>, U. Krüner<sup>18</sup>, S. Kullander<sup>15</sup>,  
U. Landgraf<sup>3</sup>, F. Lettenström<sup>12</sup>, T. Lindqvist<sup>15</sup>, G.K. Mallot<sup>7</sup>, C. Mariotti<sup>14</sup>,  
G. van Middelkoop<sup>2,10</sup>, Y. Mizuno<sup>4h)</sup>, J. Nassalski<sup>16</sup>, D. Nowotny<sup>4</sup>, N. Pavel<sup>18i)</sup>, H. Peschel<sup>18j)</sup>,  
C. Peroni<sup>14</sup>, U. Pietrzyk<sup>18k)</sup>, B. Povh<sup>4,5</sup>, R. Rieger<sup>7</sup>, K. Rith<sup>4</sup>, K. Röhrich<sup>7l)</sup>, E. Rondio<sup>17</sup>,  
L. Ropelewski<sup>17</sup>, A. Sandacz<sup>16</sup>, C. Scholz<sup>4</sup>, R. Schumacher<sup>13m)</sup>, U. Sennhauser<sup>13n)</sup>, F. Sever<sup>10</sup>,  
T.-A. Shibata<sup>5</sup>, M. Siebler<sup>1</sup>, A. Simon<sup>4</sup>, A. Staiano<sup>14</sup>, G. Taylor<sup>11p)</sup>,  
M. Treichel<sup>4q)</sup>, J.L. Vuilleumier<sup>9</sup>, T. Walcher<sup>7</sup>, K. Welch<sup>6</sup>, R. Windmolders<sup>8</sup>

(To be submitted to Physics Letters)

## ABSTRACT

We present results on inelastic  $J/\psi$  production from muon interactions with hydrogen and deuterium at an incident muon energy of 280 GeV. The measured cross section ratio per nucleon for muon-induced  $J/\psi$  production in deuterium and hydrogen was found to be  $R(D_2/H_2) = 1.01 \pm 0.15$ . The Colour Singlet model is shown to provide a good description of the observed differential cross section apart from a normalisation factor. The comparison between the observed cross section and the Colour Singlet model prediction allows the extraction of the gluon structure function  $G(x)$  of the nucleon. The momentum fraction  $x$  of the nucleon carried by the gluon is measured in the range of  $x = [0.02, 0.30]$ . The normalised gluon distribution of free nucleons thus found can be parametrised as:  $xG(x) = \frac{\eta+1}{2}(1-x)^\eta$ , with  $\eta = 5.1 \pm 0.9$  (stat.).

- + Supported by Bundesministerium für Forschung und Technologie.
- ++ Supported in part by FOM, Vrije Universiteit Amsterdam and NWO.
- \* Supported by CPBP.01.06.
- \*\* Supported by CPBP.01.09.

- a) Now at TRIUMF, Vancouver, BC, Canada.
- b) Now at Trasys, Brussels, Belgium.
- c) Now at PSI, Villigen, Switzerland.
- d) Now at CEBAF, Newport News, VA, U.S.A.
- e) Now at CERN, Geneva, Switzerland.
- f) Now at University of Mainz, Mainz, Germany.
- g) Now at Laboratoire de l'Accélérateur Linéaire, Université de Paris-Sud, Orsay, France.
- h) Now at Osaka University, Osaka, Japan.
- i) Now at DESY, Hamburg, Germany.
- j) Now at Gruner and Jahr AG & CoKG, Itzehoe, Germany.
- k) Now at MPI für Neurologische Forschung, Köln, Germany.
- l) Now at IKP2-KFA, Jülich, Germany,
- m) Now at Carnegie Mellon University, Pittsburgh, U.S.A.
- n) Now at EMPA, 8600 Dübendorf, Switzerland.
- o) On leave of absence from Jozef Stefan Institut, Ljubljana, Yugoslavia,  
now at DPhN Saclay, Gif-sur-Yvette, France.
- p) Now at University of Melbourne, Parkville, Victoria, Australia.
- q) Now at Université de Neuchâtel, Neuchâtel, Switzerland.

Deep inelastic lepton scattering (DIS) experiments provide information about the structure of the target hadrons. This substructure can be interpreted in terms of partons. From inclusive lepton scattering experiments it is known that half of the nucleon momentum is carried by charged partons [1]. In the quark-parton description, the other half of the nucleon momentum is considered to be carried by gluons.

The  $J/\psi$  production in DIS (fig. 1a) can be related to the gluon distribution in the nucleon via the process of photon-gluon fusion [2,3,4,5,6]. In the Colour Singlet model (CS) [4,5,6] the  $J/\psi$  is represented by a definite wave function of the  $c\bar{c}$  system, which describes a colour singlet state with  $J^P = 1^-$  and the  $J/\psi$  rest mass [4]. In this model, the amplitudes of the process  $\gamma g_1 \rightarrow J/\psi g_2$  (fig. 1b) are calculated under the assumption that the virtual photon fuses with a gluon in the target nucleon and colour conservation is required explicitly. For inelastic  $J/\psi$  production, the gluons  $g_1$  and  $g_2$  are hard enough for the effects of multiple soft gluon emission to be negligible [4]. Since the initial gluon carries a small fraction of the nucleon momentum, the  $J/\psi$  is produced in the forward rapidity region in the photon-nucleon centre-of-mass frame.

Diffraction photoproduction of vector mesons lighter than the  $J/\psi$  is often interpreted in terms of Vector Meson Dominance (VMD) [7]. The VMD model has been extended to give a description of non-diffractive and inelastic  $J/\psi$  production by including the Drell-Yan mechanism (DY) [8,9]. In this process, the photon couples to a light vector meson which then interacts with the target nucleon and produces a  $J/\psi$  via a DY-like process in which the time-like photon is replaced by a gluon which couples to a  $J/\psi$  (fig. 1c). The light vector meson and the target nucleon contribute equally to its momentum. This causes the rapidity distribution of the  $J/\psi$  to be centred around zero in the photon-nucleon centre-of-mass system. This behaviour is distinctly different from that given by the CS model.

In this paper we present differential cross sections for  $J/\psi$  production obtained from  $\mu^+$  interactions with hydrogen and deuterium at an incident energy of 280 GeV. The kinematics of the  $J/\psi$  production process was reconstructed from the detection of both  $J/\psi$  decay muons together with the incident and scattered muon (fig. 1a).

The experiment was performed in the M2 muon beam at the CERN SPS using an upgraded version of the EMC forward spectrometer [12]. The target system was composed of two complementary sets of targets, each consisting of two 3 m long target vessels filled with liquid hydrogen and deuterium respectively. The two sets differed only in the ordering of the vessels with respect to the beam direction. Both sets were exposed alternately to a beam of 280 GeV muons. The beam intensity was monitored by a dedicated beam trigger. With this trigger the integrated effective incident muon flux was measured to be  $(3.05 \pm 0.06) \times 10^{12}$ , corresponding to a total luminosity of  $125 \text{ pb}^{-1}$ . Data were collected using the standard single arm trigger (T1) which accepted muons with scattering angles larger than 10 mrad. Events with three or more outgoing tracks were selected in the analysis also including tracks at angles smaller than 10 mrad. The invariant mass of any pair of oppositely

charged particles was calculated for each event. In order for the event to be accepted two conditions for these track pairs had to be fulfilled: i) at least one particle had to be identified as a muon in our apparatus and ii) the invariant mass of the pair had to be consistent with the  $J/\psi$  mass. The scattered muon was selected from the remaining reconstructed tracks with the same charge as that of the incident muon. In 10% of the events more than one candidate for the scattered muon was found. These events were subjected to a further selection in which the muon with the highest energy was chosen whenever its energy was at least 50% higher than the energy of any other candidate. Otherwise, the track with the smallest scattering angle was taken. For this class of events Monte Carlo studies showed that the scattered muon was misidentified in less than 10% of the cases using these criteria.

The relevant kinematical variables are defined in table 1 together with the cuts applied in the present analysis. The cuts were optimised so as to minimise the background and to exclude regions of poor acceptance. The upper cut on  $z$  and the lower cut on  $P_T^2$  ensured that the  $J/\psi$  production is inelastic and incoherent.

<b>Table 1</b> Kinematic variables of the $J/\psi$ production process			
$-Q^2 = q^2$			Invariant mass squared of the virtual photon.
$\nu = \frac{q \cdot p_N}{M_N}$	$\stackrel{\text{LAB}}{=} E_\mu - E_{\mu'}$		Energy of the virtual photon.
$z = \frac{p_{J/\psi} \cdot p_N}{q \cdot p_N}$	$\stackrel{\text{LAB}}{=} \frac{E_{J/\psi}}{\nu}$		Elasticity parameter of the $J/\psi$ production process.
$P_T^2 =  \vec{p}_{J/\psi} ^2 - \frac{(\vec{p}_{J/\psi} \cdot \vec{q})^2}{ \vec{q} ^2}$			Transverse momentum squared of the $J/\psi$ meson with respect to photon direction.
Applied cuts in the event selection			
	15 GeV	$\leq$	$E_{\mu'}$
	10 GeV	$\leq$	$E_{\text{decay muon}}$
	60	$\leq$	$\nu \leq 240$ GeV
	0.2	$\leq$	$z \leq 0.9$
	0.1	$\leq$	$P_T^2 \leq 10$ (GeV/c) <sup>2</sup>
Invariant mass cut			
	2.90	$\leq$	$M_{\mu^+\mu^-} \leq 3.30$ GeV/c <sup>2</sup>

Figure 2 shows the invariant mass  $M_{\mu^+\mu^-}$  distribution of the selected track pairs. The sum of a gaussian distribution and an exponentially falling background was fitted to the mass spectrum obtained for hydrogen and for deuterium (smooth curves in fig. 2). The  $J/\psi$  signal from hydrogen and deuterium was given by the sum of the events in the defined mass interval (see table 1) from which the background events parametrised by the exponential curve had been subtracted. This yielded  $85 \pm 10$  and  $194 \pm 15$  events for the hydrogen and deuterium respectively. The average fitted value of the peak position was found to be  $3093 \pm 5$  MeV/c<sup>2</sup>. The width of the gaussian distribution corresponds to the experimental momentum resolution of 1%.

The ratio of the cross sections per nucleon for muon-induced  $J/\psi$  production in deuterium and hydrogen was found to be  $R(D_2/H_2) = 1.01 \pm 0.15$ . The quoted error is statistical only. Geometrical acceptance and efficiency corrections cancel in the calculation of the ratio as do the integrated beam fluxes. The frequent exchange of the target sets also minimises the effects of possible time dependent changes in the apparatus acceptance and efficiency. The systematic error on the ratio of target densities was estimated to be less than 1%. The effect of radiative corrections on the ratio was estimated to be small compared to the statistical error. The result is consistent with equal  $J/\psi$  production rates for neutron and proton. The hydrogen and deuterium data were therefore combined in the subsequent analysis, resulting in 279 reconstructed  $J/\psi$  events and 41 background events.

To obtain absolute cross sections from the experimental counting rates, the acceptance was calculated using a Monte Carlo simulation including a complete description of the apparatus and detector efficiencies. The Monte Carlo events were subjected to the same analysis procedure as the real data events. The branching ratio of the  $J/\psi$  decay into  $\mu^+\mu^-$  was taken to be  $6.9 \pm 0.9$  % [23]. Radiative effects on the measured cross sections give rise to small corrections, typically 5% or less [20,21]. Although the mass resolution is good enough to separate the  $J/\psi$  signal from heavier  $c\bar{c}$  resonances, different sources of charm production can contribute to the observed signal strength. The contribution to the observed inelastic  $J/\psi$  signal through  $\psi'$  production and subsequent decay was estimated to be less than 15%, assuming that the cross section of  $\psi'$  production is 20% of that of  $J/\psi$  production [13] and taking into account the known branching ratio of 0.57 for  $\psi'$  decay into  $J/\psi$  [23]. The measured cross section was not corrected for the above-mentioned effects. Only statistical errors are given; the combined systematic error due to the uncertainty on the target densities and the integrated muon flux was estimated to be less than 2%.

Figure 3 shows the observed differential cross section  $d\sigma(\mu N \rightarrow \mu' J/\psi X)/dy$ . The rapidity  $y$  of the  $J/\psi$  is defined as  $y = 1/2 \ln([E+p_{//}]/[E-p_{//}])$ , where  $E$  and  $p_{//}$  are the  $J/\psi$  energy and longitudinal momentum with respect to the virtual photon calculated in the photon-nucleon centre-of-mass system. The  $J/\psi$  production is clearly peaked in the forward direction.

The dashed line in fig. 3 represents the prediction of the VMD model in combination with the DY mechanism for an incident energy of 280 GeV. The calculation was performed using eq. (3) of ref. [8], to which a multiplicative factor of 1/8 was applied, representing the fraction of  $c\bar{c}$  pairs going to  $J/\psi$  [2]. The muoproduction cross section was obtained from the photoproduction cross section by multiplication with the virtual photon flux factor [8] computed following the convention introduced by Hand [16]. The cross section of the subprocess  $q\bar{q} \rightarrow J/\psi$  was integrated from the charm quark mass threshold up to the D-meson mass [2]. Values for the input parameters were taken from ref. [23], with the strong coupling constant chosen to be  $\alpha_s(M_{J/\psi}^2) = 0.3$ , the charm quark mass  $m_c = 1/2 M_{J/\psi}$  and the quark distributions taken from ref. [8]. Although our apparatus accepts only events with positive rapidity, it is clear that the computed distribution cannot account for the signal strength for  $y \geq 1$ .

The solid line in fig. 3 represents the prediction of the CS model for inelastic and incoherent  $J/\psi$  production. For comparison with the data a normalisation factor of 2.4 was applied. The calculation was performed according to ref. [17], with a QCD radiative correction factor to the leptonic width  $\Gamma_{\mu^+\mu^-}(J/\psi)$  of  $(1-16\alpha_s(M_{J/\psi}^2)/3\pi)$  [18]. Values for the input parameters used in the present calculation were taken from ref. [23], with the same value for  $\alpha_s(M_{J/\psi}^2)$  and  $m_c$  as in the VMD+DY calculation and a gluon distribution  $G(x) = 3/x(1-x)^5$ . From fig. 3 it can be seen that the cross section of  $J/\psi$  production as a function of the rapidity is well described by the CS model. The QCD radiative correction to the leptonic width takes into account half of the previously measured discrepancy of a factor of 5 between model and data [5,10]. In the present analysis however, the CS model still underestimates the observed signal by a factor of 2.4. Note that the normalisation of the CS model is sensitive to the mass of the charm quark and proportional to the square of the strong coupling constant [4]. Furthermore, the calculation of the cross section is performed by using a non-relativistic description of the  $c\bar{c}$  bound state. It is expected that relativistic effects might distort this description through corrections of order  $\sqrt{1-\beta^2}$ , with  $\beta$  estimated to be 0.5 [19].

The normalised differential cross section  $2\pi/\sigma d\sigma(\mu N \rightarrow \mu' J/\psi)/d\phi$ , where  $\phi$  is the azimuthal angle between the muon scattering plane and the  $J/\psi$  production plane, is shown in fig. 4. The solid curve is a fit of the function  $(1+B\cos\phi+C\cos 2\phi)$  to the measured distribution. The results of the fit are given in table 2 together with the CS model predictions for scalar and vector gluons [11].

Table 2			
The azimuthal angle distribution $(1+B\cos\phi+C\cos2\phi)$			
Experimental Results		CS Model ( $\langle Q^2 \rangle = 1.5 \text{ GeV}^2$ )	
		$J_{\text{gluon}}^P = 0^+$	$J_{\text{gluon}}^P = 1^-$
B =	- 0.13 ± 0.08	+ 0.12	- 0.14
C =	- 0.02 ± 0.08	- 0.11	- 0.08

The results, when compared with the predictions of the CS model computed at the average  $Q^2$  of the data ( $1.5 \text{ GeV}^2$ ), are consistent with  $J^P = 1^-$  for the gluon. The same results disfavour the description of  $J/\psi$  production as presented in ref. [3], in which the predictions of the model [2] are extended to second order terms without explicit colour conservation.

Since the CS model provides a good description of our data it has been used to extract the gluon distribution of free nucleons. The measured differential cross section  $d\sigma(\mu N \rightarrow \mu' J/\psi X)/dx$ , with  $x = \hat{s}/s$  where  $\hat{s}$  and  $s$  are the centre-of-mass energies in the photon-gluon and the photon-nucleon reference frames, was divided by that calculated in the CS model [6,20]. In the latter, the gluon distribution  $xG(x)$  was set to unity. The variable  $x$  given in the CS model by  $x = 1/s [M_{J/\psi}^2/z + P_T^2/z(1-z)]$  can be interpreted as the momentum fraction of the nucleon carried by the probed gluon. The function  $c \frac{\eta+1}{2} (1-x)^\eta$  was fitted to the data; the result of the fit was  $c = 2.4 \pm 0.4$  and  $\eta = 5.1 \pm 0.9$ . The value of  $c$  corresponds to the previously introduced normalisation factor and  $\eta$  represents the shape of the gluon distribution. The extracted normalised gluon distribution is shown in fig. 5 together with its parametrisation  $xG(x) = \frac{\eta+1}{2} (1-x)^\eta$ . The results of EMC from the analysis of  $J/\psi$  production on  $\text{NH}_3$  [20], also shown in fig. 5, are in good agreement with the present data.

Gluon distributions have also been obtained previously from QCD analyses of structure function measurements. These yield parametrisations that allow a large spread of  $\eta$  values ranging from 3 to 11 [22]; this uncertainty in  $\eta$  has been discussed in ref. [24].

In the present work we have shown that the CS model is able to describe inelastic  $J/\psi$  production and consequently that it is possible to extract the gluon distribution directly.

## References

1. T. Sloan, G. Smadja and R. Voss, Phys. Rep. **162** (1988) 45.
2. T. Weiler, Phys. Rev. Lett. **44** (1980) 304.
3. D.W. Duke and J.F. Owens, Phys. Rev. **D23** (1981) 1671.
4. E.L. Berger and D. Jones, Phys. Rev. **D23** (1981) 1521.
5. R. Baier and R. Rückl, Nucl. Phys. **B201** (1982) 1 ;  
R. Baier and R. Rückl, Nucl. Phys. **B218** (1983) 289.
6. A.D. Martin, C.-K. Ng and W.J. Stirling , Phys. Lett. **191B** (1987) 200.
7. T.H. Bauer , R.D.Spital, D.R.Yennie and F.M.Pipkin , Rev. Mod. Phys. **50** (1978) 261;  
K. Schilling, P. Seyboth and G. Wolf, Nucl. Phys. **B15** (1970) 397.
8. J.P. Leveille and T. Weiler, Phys. Lett. **86B** (1979) 377.
9. S.D. Drell and T.M. Yan, Ann. Phys. **66** (1971) 578.
10. EMC, J.J. Aubert et al., Nucl. Phys. **B213** (1983) 1.
11. J.G. Körner, J. Cleymans, M. Kuroda and G.J. Gounaris, Phys. Lett. **114B** (1982) 195.
12. NMC, D. Allasia et al., CERN Report CERN-PPE/90-103 and references cited therein.
13. R. Barate et al., Z. Phys. **C33** (1987) 505.
14. E.L. Berger and D. Jones, Phys. Lett. **121B** (1983) 61.
15. EMC, M. Arneodo et al., Z. Phys. **C35** (1987) 1.
16. L.N. Hand, Phys. Rev. **129** (1963) 1834.
17. K.J. Abraham, Phys. Lett. **240B** (1990) 224;  
K.J. Abraham, private communication.
18. R. Barbieri, R. Gatto and E. Remiddi, Phys. Lett. **106B** (1981) 497.
19. P.B. MacKenzie and G.P. Lepage, Phys. Rev. Lett. **47** (1981) 1244;  
G.P. Lepage, S.J. Brodsky, T. Huang and P.B. MacKenzie, SLAC and  
Cornell report LNS-82/522, Banff Summer Inst. on Particle Physics 1981;  
W. Buchmüller and S.-H.H. Tye, Phys. Rev. **D24** (1981) 132.
20. N. Dyce, Ph.D. thesis, Lancaster University (1988).
21. L.W. Mo and Y.S. Tsai, Rev. Mod. Phy. **41** (1969) 205;  
Y.S. Tsai, SLAC-PUB-848 (1971).
22. EMC, J.J. Aubert et al., Nucl. Phys. **B272** (1986) 158;  
BCDMS, A.C. Benvenuti et al., Phys. Lett. **B223** (1989) 490.
23. Review of Particle Properties, Phys. Lett. **B239** (1990).
24. J. Feltesse, Proceedings of the XIV International Symposium on Lepton and Photon Interactions,  
Stanford, August 6-12, 1989, editor M. Riordan.



## Figure Captions

- Fig. 1 Diagrams for muon induced  $J/\psi$  production.  
a) The kinematics of the reaction.  
b) The Colour Singlet model [4].  
c) The Vector Meson Dominance model with the Drell-Yan mechanism [8,9].
- Fig. 2 Invariant mass distribution of selected  $\mu^+\mu^-$  pairs for deuterium and hydrogen. The smooth curves are the sum of a gaussian and an exponentially falling background fitted to the observed distributions.
- Fig. 3 Cross section for  $J/\psi$  muoproduction as a function of the rapidity. The solid curve shows the CS model prediction and the dashed curve shows that of the VMD model in combination with the DY mechanism.
- Fig. 4 Normalised muoproduction cross section as a function of the azimuthal angle  $\phi$  between the muon scattering plane and the  $J/\psi$  production plane. The solid curve is a fit of the function  $[1+B\cos\phi + C\cos2\phi]$  to the observed distribution.
- Fig. 5 The nucleon gluon distribution  $xG(x)$  from the present experiment and ref. [20]. The solid curve is a parametrisation of  $xG(x)$  discussed in the text.

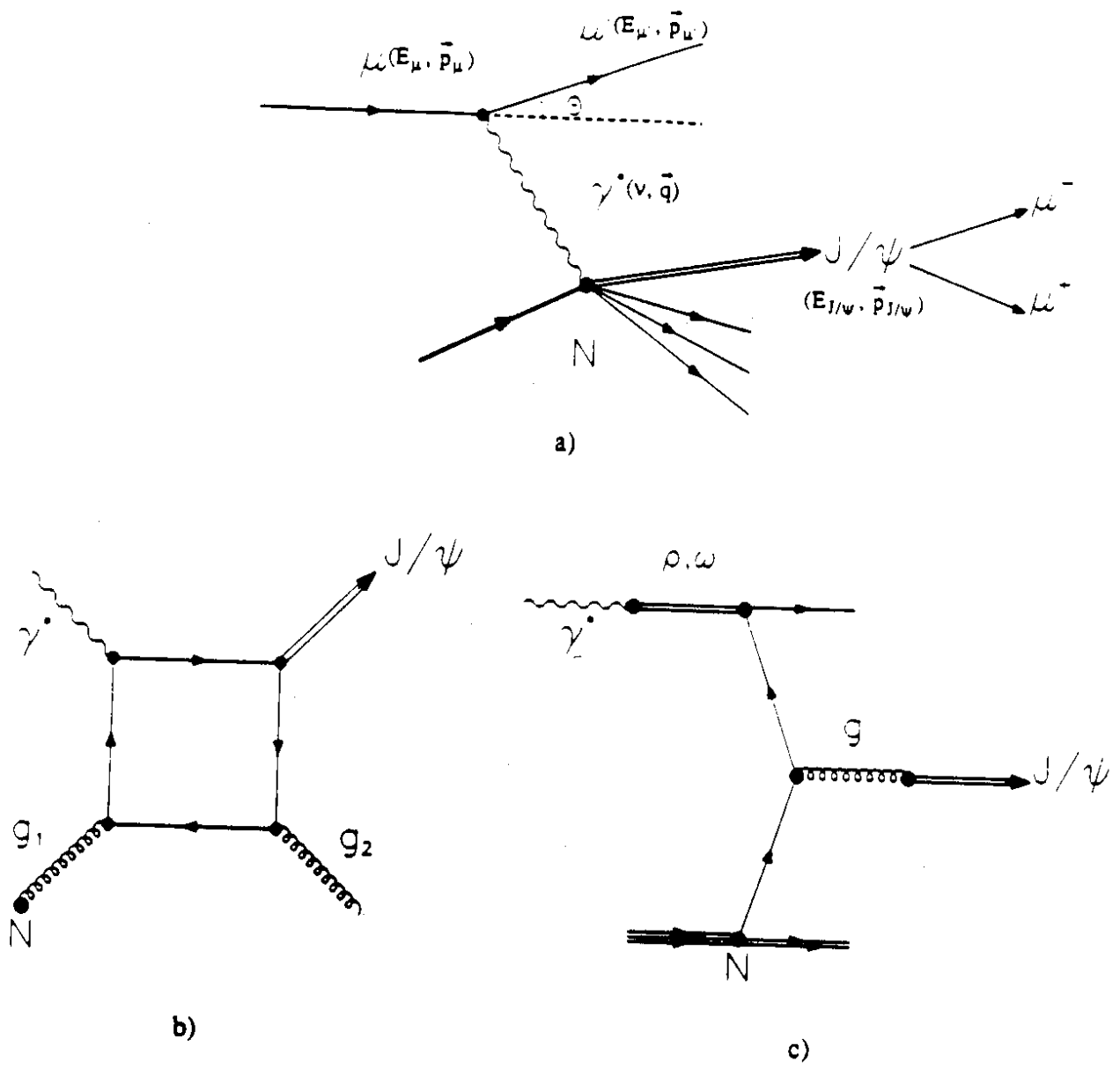


FIG. 1

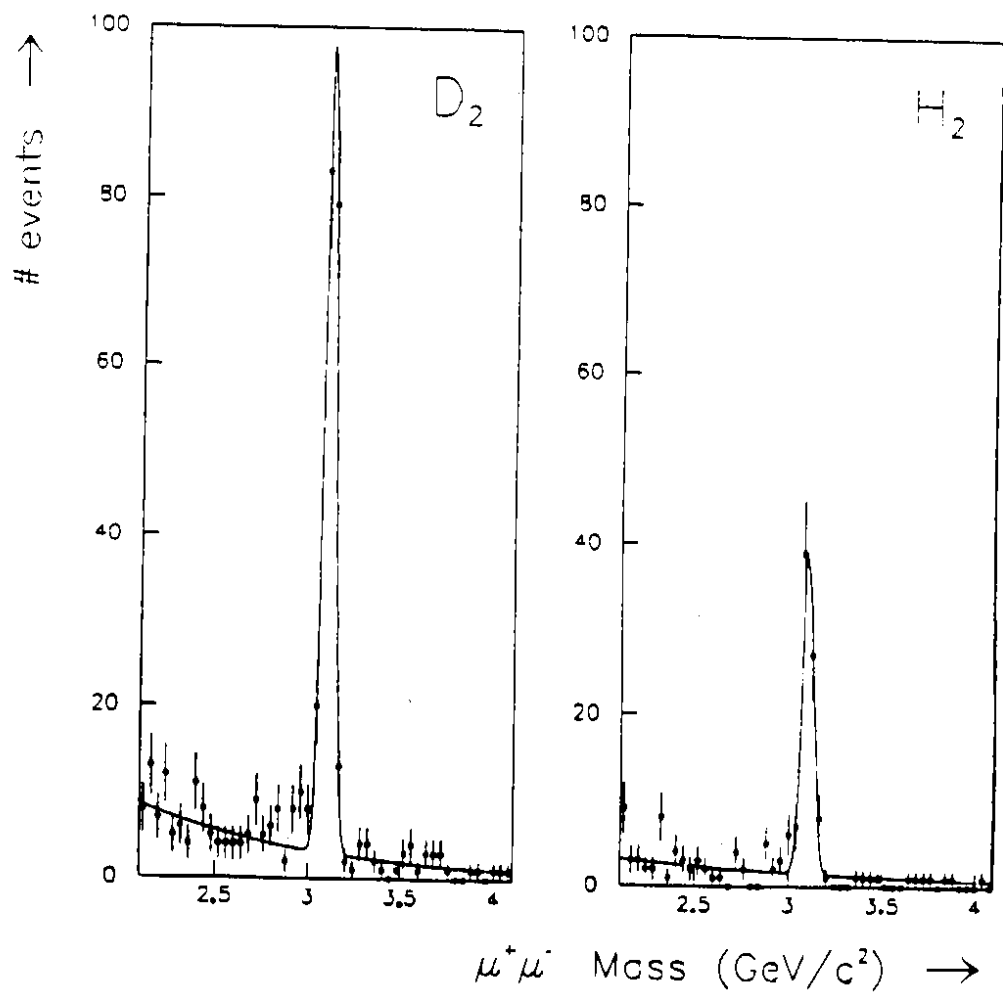


FIG. 2

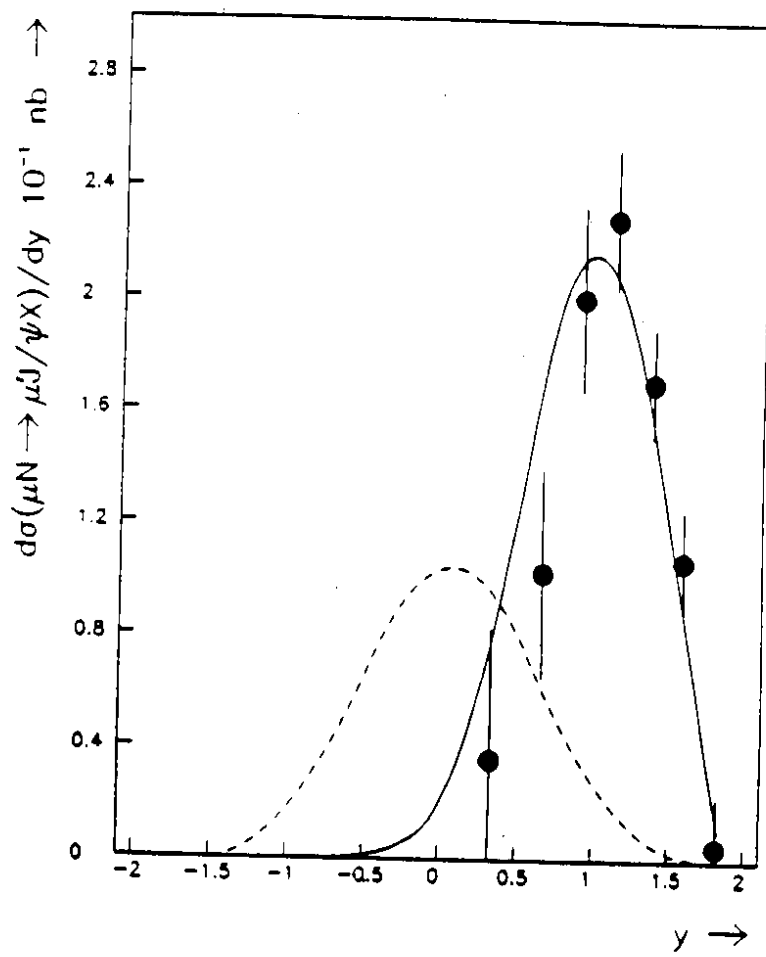


FIG. 3

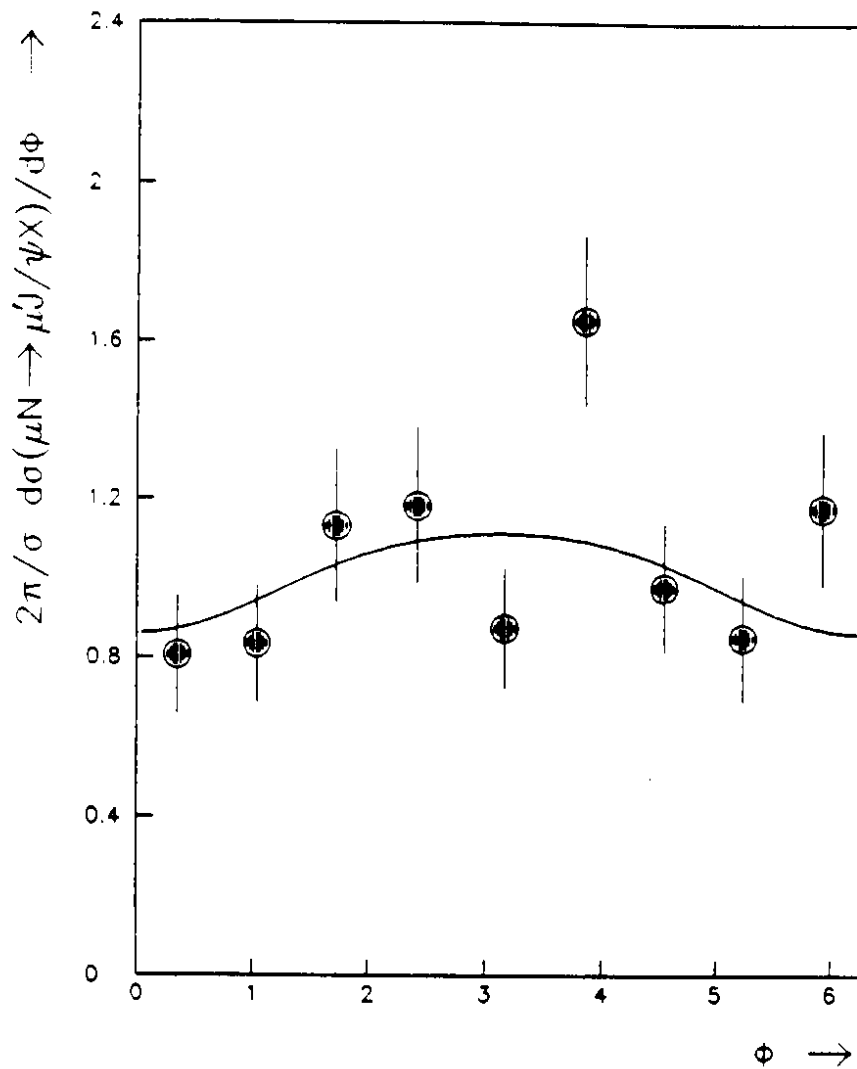


FIG. 4

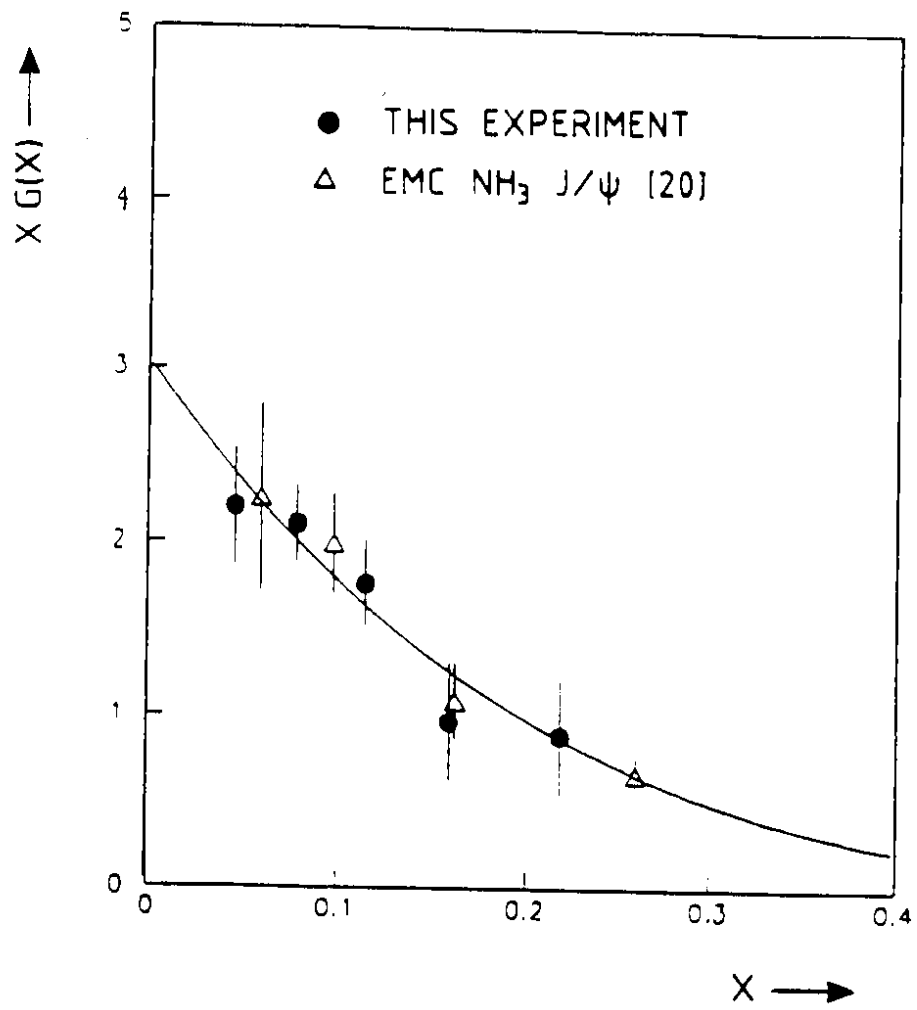


FIG. 5